Journal of Materials and Electronic Devices 3 (2021) 8-14

Investigation of CuAlNi Shape Memory Alloy Doped with Graphene

Oktay KARADUMAN[1], Canan Aksu CANBAY[1*]

[1]Department of Physics, Science Faculty, Firat University, Elazig, 23119, TURKEY

In the research area of shape memory alloys (SMAs), which are one of the most utilized class of smart materials, many additive alloying metal elements have been incorporated into shape memory alloy systems to improve or modify their functional and characteristic properties such as to get higher or lower martensitic transformation temperatures, to enhance shape recovery or superelasticity capabilities, to improve ductility or strength etc. Though the additive elements are often metals, some other materials can be added in SMA systems, too. Cu-based SMAs are regarded as the most potential alternative to the superior but expensive NiTi SMAs. Therefore, improving the SMA features of the Cu-based SMAs by some methods (such as doping additive elements into them, fabricating them by different production routes, etc.) have also become very attractive to the researchers who work in this area. In this experimental study, ternary CuAlNi shape memory alloy was doped by minor amount of pure graphene (in the form of nanoplatelets) via melting in vacuum arc melter under argon plasma. The alloy obtained in as-cast ingot form was cut into small pieces suited for a series of differential calorimetric and structural shape memory effect characterization measurements. Before conducting the tests, all of the alloy samples were solution-treated in high β–phase temperature region and instantaneously quenched in iced-brine water. By doing this fast cooling, the hypoeutectoid precipitations of α (Cu) and γ2 (Al) were surpassed and thus the β1’ martensite phase formed in the alloy texture, which phase constitutes the ground for a shape memory effect property to form in the alloys. Then, the alloys chemical composition was determined by EDX test result showing the presence of carbon content in the alloy. Thermal characterization tests were performed by DSC and DTA measurements taken at varying heating/cooling rates under inert argon athmosphere. The cyclic thermograms obtained by these thermal tests revealed the endothermic and exothermic martensitic transformation peaks occurred above 100 °C indicating the presence of shape memory effect property in the alloy. The structural X-ray diffraction test was carried out at room temperature at where the alloy was in martensite phase, expectedly the diffraction peaks formed by reftection of X-rays from the atomic planes of β1’ martensite structures were observed on the diffraction pattern of the alloy.

Keywords: *Graphene doped CuAlNi SMA, Martensit, Shape memory effect, DSC, DTA, X-ray diffraction*

Submission Date: 22 April 2021
Acceptance Date: 21 July 2021

**Corresponding author: caksu@firat.edu.tr*

1. Introduction

For a few decades the cost effective Cu-based shape memory alloys (SMAs) have been studied by many researchers to develope an alternative to the superior NiTi-based SMAs which are the most commercial but also the most expensive SMAs as compared with other SMAs [1-4]. Regarded as the closest competitor of NiTi SMAs, Cu-based

SMAs (e.g. CuAlNi, CuAlMn) aroused interest for their good shape recovery, advantageous low costs, fabrication ease, and excellent damping, thermal and electrical conductivity properties [2-4,5]. On the other hand, brittleness, thermal stability, and mechanical strength problems that stem from microstructural features are disadvantages of Cu-based SMAs [2-4].

Tuning chemical compositions or adding extra alloying elements, producing by different fabrication methods or applying thermomechanical treatments are known as the most used methods [2-4, 6-15] to improve or modify the properties or performances of SMAs upon demands in SMA related industries.

Among Cu-based SMAs, CuAlNi SMAs are preffered due to their outstanding shape memory effect (SME) and superelasticity (SE), improved mechanical properties and high thermal stability at temperatures above 100°C, especially for high temperature shape memory alloy (HTSMA) applications [2,4,16]. Previously, different grain refining additive metal elements such as Ti, Mn, B, Ce, Co, V or Zr [1,2,4,9,17] were infused (doped) into the ternary CuAlNi base SMAs.

It's been confirmed that nanoparticles can improve the thermomechanical and structural properties of metals without damaging their plasticity. Infusing metals and alloys with nanoparticles [18, 19, 20, 21] can change or improve their thermal stability, strength, stiffness, plasticity, corrosion resistance and durability under high temperatures. In literature, there are very few reports on doping SMAs with carbon and carbon nanomaterials [20, 21, 22, 23]. Among these, Saud *et al.* [23] doped a CuAlNi SMA (having composition of 83.8Cu-11.5Al-4.5Ni wt.%) with a minor amount (0.2 wt.%) of carbon nanotubes (CNTs) having a tube shape diameter of 34–55 nm and reported that the addition of CNTs substantially affected on the shape recovery ratio, martensitic microstructure, phase transformation temperatures and related thermodynamic parameters. They also stated that the CNTs addition increase the dislocations in the alloy matrix which enhances shape memory effect.

In the available literature, there is no any report on SMAs doped with graphene (with the exception of the works like coating of graphene on SMAs or other). In this work, the graphene nanoplatelets with 5 nm of size was infused into the CuAlNi SMA via arc melting method and the shape memory effect and related mirostructural properties of the produced alloy was investigated.

2. Experimental

The graphene (C) doped CuAlNi-C shape memory alloy with an unprecedented composition of 73.18Cu-20.47Al-3.75Ni-2.49C as at.% (or 85.25Cu-10.13Al-4.04Ni-0.55C as wt.%) was prepared from powders of high purity (99.9%) Cu, Al, Ni metal elements and graphene nanoplatelets. The powder of graphene nanoplatelets with purity of 99.9+%, size of 5 nm, specific surface area (S.A.) of 170 m^2/g, and diameter of 18 μm was purchased from Nanografi Nanotechnology AS company. All powders were balanced as to alloy composition and mixed together and then this powder mixture was pelletized under pressure. Then the obtained pellets were melted by an Edmund Buehler Arc Melter under inert argon gas plasma atmosphere and, as it turned out, the CuAlNi-C alloy was obtained as-cast ingot. Then, the minikin (~30-60 mg) tablet shaped alloy pieces as test specimens were prepared by cutting from that ingot and all of these alloy samples were together solution-treated in high β-phase temperature region (at 900 °C) for 1 hour. From this high temperature they were rapidly cooled down by quenching them into iced-brine water medium to surpass the hypoeutectoid precipitating and thus to make way for the formation of β1' martensite phase in the alloy texture, in other words to endow the alloy its shape memory effect property. The chemical composition and SEM image of the alloy were obtained at room temperature via a Zeiss Evo MA10 model EDX (energy dispersive X-ray) instrument. The characteristic martensitic transformation peaks with analyzed data and the thermal behavior extending over high temperature β-phase region of the alloy were detected by using of a Shimadzu DTG-60AH model differential thermal analysis (DTA) instrument run at escalating heating/cooling rates of 25, 35 and 45 °C/min between room temperature and 900 °C. The XRD test (with CuKα radiation) taken at room temperature was carried out by using a Rigaku RadB-DMAX II diffractomer to pick out the X-ray diffraction peaks of the atomic planes of the alloy.

3. Results and Discussion

The SEM image with EDX composition result for the CuAlNi-C alloy is presented in Fig.1. Here, the minor amount of carbon (graphene) content with a concomitant and much lesser oxygen entity (which might have occurred either by oxidation of graphene and alloying metal elements) was observed. On the SEM image of the alloy surface, the regions of homogeneously disseminated dark graphene spots [24] like small disintegrated precipitates and other precipitates can be seen. The chemical composition of the CuAlNi-Graphene alloy sample was detected as $_{73.18}$**Cu**-$_{20.47}$**Al**-$_{3.75}$**Ni**-$_{2.49}$**C** in at.% (or $_{85.25}$Cu-$_{10.13}$Al-$_{4.04}$Ni-$_{0.55}$C in wt.%). The very small oxygen content might have formed mostly on the alloy surface by oxidation bonding with either graphene and alloying metal elements during production and testing processes.

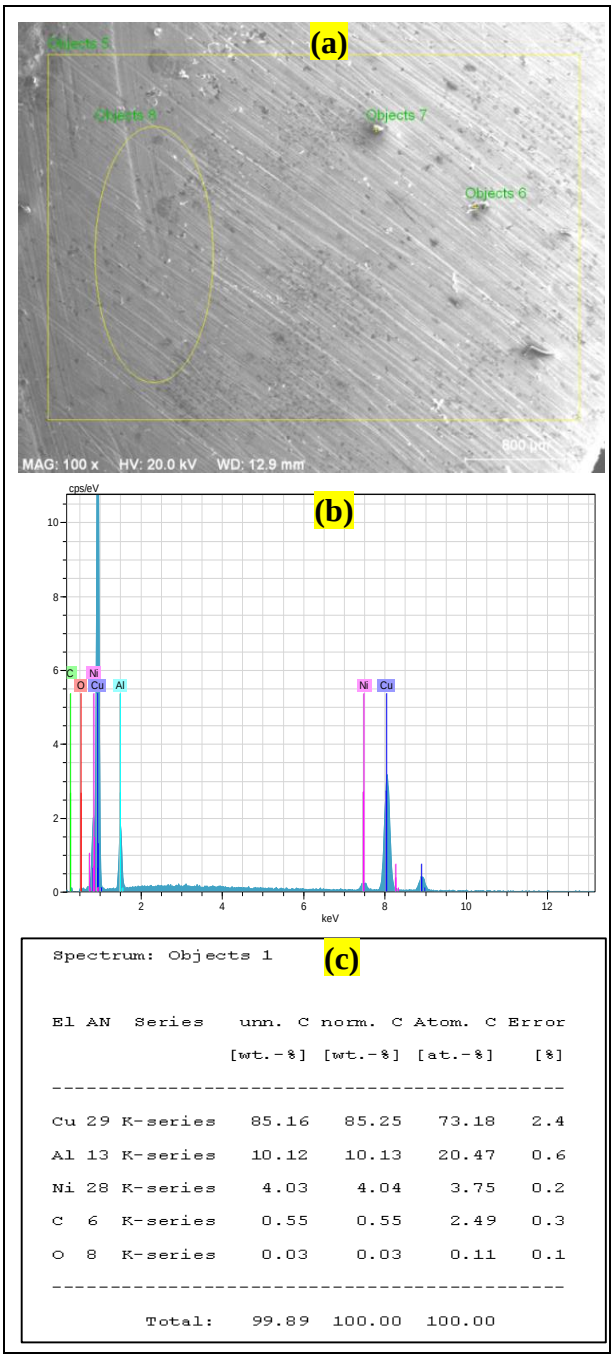

Fig.1. (**a**) The SEM image with (**b**, **c**) EDX result of the CuAlNi-C alloy obtained in room conditions.

The DTA curves (thermograms) of CuAlNi-C alloy obtained at the escalating heating/cooling rates of 25, 35 and 45 °C/min are given in Fig.2. On all of these DTA curves, the peaks of the each reversible martensitic phase transitions (austenite ↔ martensite) pair can be seen and indicate the shape memory effect property of alloy. On the each heating fragment of these curves, from far left room temperature to the far right high β-phase temperatures, there is seen multistage phase transitions that goes like this; β1'(martensite)→β1(austenite, $DO_3/L2_1$)→ B2(metastable) →hypoeutectoid precipitations (α+γ2)→eutectoid dissolution (of the precipitates)→B2(ordered)→ A2(disordered) and this multiple phase transition chain is a common behavior of Cu-based alloys [13-15, 25].

By making peak analyses on the martensitic (M↔A) transformation peaks, these were automatically done by DTA analysis program which calculates peak areas and determines start, finish, max or min peak values (temperatures) by using tangent differentiation method, the characteristic martensitic phase start and finish transformation temperatures; A_s and A_f for martensite to austenite (M→A) peaks, and M_s and M_f for austenite to martensite (A→M) peaks, A_{max} temperatures and the enthalpy change ($\Delta H_{M\leftrightarrow A}$) values of these peaks were directly obtained and listed in Table-1. As seen in the Table-1, the characteristic transformation temperatures on average were found to be located between ~190-379 °C, which acordingly categorizes the produced CuAlNi-C alloy as a high temperature shape memory alloy (HTSMA) [12,13,14,16,23]. Although found compatible with the previously reported characteristic transformation temperatures (btw. ~225-241°C) of the CuAlNi-CNTs alloy [23] because both are in the same temperature interval, the characteristic transformation temperatures of the produced CuAlNi-C HTSMA here were found much more extended than those of the reported work [23]. This great difference shows itself better by making a comparison of hysteresis gap (A_s-M_f) values (seen in Table-1) of the graphene-doped alloy (produced in this work) having an average hysteresis gap of ~111 °C and the previously worked CNTs-doped alloy [23] having a hysteresis gap of ~12 °C. Such a large difference between the two hysteresis gap maybe resulted from the difference between the thickness values of both dopant materials of graphene nanoplatelets (with 5 nm) and CNTs nanotubes (with 35-55 nm) or/and also maybe from the little difference between their amounts used in alloying. The dopant graphene nanoplatelets with 5 nm thickness and 18 μm lateral sheet diameter distributed through the alloy matrix act like interfaces of short grain borders with high energies between graphene and CuAlNi base alloy texture, and these interfaces between graphene and intermetalic alloy phases can reduce the speed of heat transfer and cause a delayment in the eventuating of both two opposite way of transformations i.e. a large hysteresis gap. The hysteresis gap (A_s-M_f) values, the values of the other calculated important kinetic parameters of equilibrium temperature (T_0) and entropy change ($\Delta S_{M\leftrightarrow A}$) values of the CuAlNi-C alloy are given in Table-1.

The thermal equilibrium temperature (T_0) values of the alloy were calculated by using $T_0=(A_f+M_s)/2$ formula [13,14]. T_0 is the temperature at where the austenite and martensite phases have the equal the Gibbs or chemical free energy (G) amounts, so there is no any driving force that can cause neither a backward nor forward martensitic phase transformation. Hereby from these T_0 values, the entropy

change ($\Delta S_{M\leftrightarrow A}$) values for the each opposite way M↔A transformation were computed using $\Delta S_{M\leftrightarrow A}=\Delta H_{M\leftrightarrow A}/T_0$ relation [13,14].

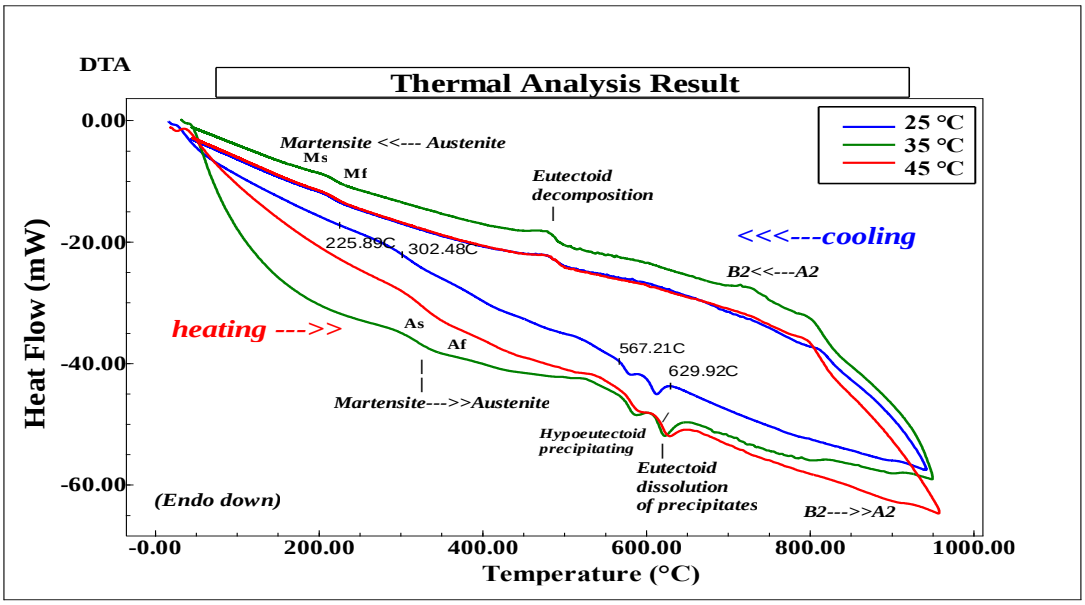

Fig.2. The DTA cyclic heating/cooling curves of CuAlNi-C alloy obtained at the heating/cooling rates of 25, 35 and 45 °C/min.

Table-1: The martensitic transformation temperatures and kinetic parameters of the CuAlNi-C SMA.

Heating/cooling rate (°C/min)	A_s (°C)	A_f (°C)	A_{max} (°C)	M_s (°C)	M_f (°C)	A_s-M_f (°C)	T_0 (°C)	$\Delta H_{M\rightarrow A}$ (J/g)	$\Delta H_{A\rightarrow M}$ (J/g)	$\Delta S_{M\rightarrow A}$ (J/g°C)	$\Delta S_{M\rightarrow A}$ (J/g°C)
25	291.49	364.91	323.36	226.59	190.30	101.19	295.75	0.89	2.40	0.00301	0.00811
35	303.37	386.49	343.73	227.90	188.96	114.41	307.19	1.30	2.56	0.00423	0.00833
45	310.14	385.73	352.63	230.63	192.72	117.42	308.18	1.62	3.17	0.00526	0.01029
Avg.	301.67	379.04	339.91	228.37	190.66	111.01	303.71	1.27	2.71	0.00417	0.00891

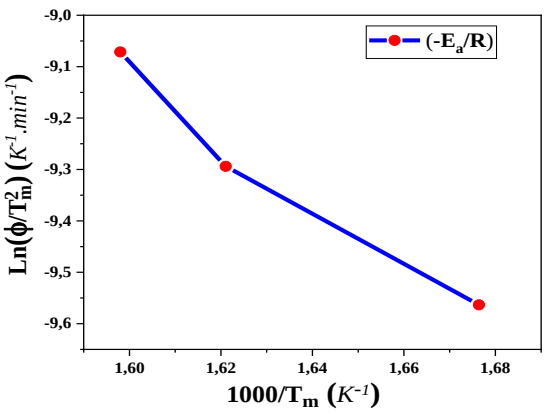

Fig.3. The activation energy (E_a) change graphic of the CuAlNi-C HTSMA.

The heating rate dependent activation energy (E_a) parameter is another important thermodynamic parameter of SMAs and for a martensitic transformation to occur this energy barrier level must be overcome. This energy affects on the crystallization configuration of the alloys. Based on the M→A peak shifts resulted from the different heating rates, the value of the E_a energy for the CuAlNi-C HTSMA can be calculated by using the well known Kissinger formula [13,26] given as below;

$$\frac{d\,[ln(\emptyset/T_m^2)]}{d(1/T_m)} = -\frac{E_a}{R} \qquad (1)$$

where; Φ refers to heating rate variable, T_m represents maximum peak temperature (A_{max}) variable, and R stands for the universal gas constant (R= 8.314 J/mol.K). To show the change in the activation energy (E_a) depending on heating rate and to obtain the left term of Eq.-1 as linear fitting slope value, a plot of $ln(\Phi/T_m^2)$ versus $1000/T_m$ was drawn as given in Fig.3. By substituting the obtained slope value of this plot

instead of the left term in the Eq.1, the E_a energy barrier level of the CuAlNi-C alloy was found as 50.01 kJ/mol.

The XRD pattern of the polycrystalline natured alloy obtained at room temperature (at where the alloy is in martensite phase) is given in Fig.4. As seen on this X-ray diffraction pattern, the highest peak belongs to the monoclinical β1'(128) martensite phase and the other observed peaks are; the monoclinical β1'(020), β1'(0022), β1'(122), β1'(0018), β1'(1210), β1'(2010), β1'(2012), β1'(208), β1'(1127), β1'(042) β1'(320) martensites, the hexagonal γ1'(111) and γ1'(221) martensites, a β1(200) [13,14,23,27,28,29,30,31,32,33]. Besides, the peaks of a graphene-oxide GO(001) and a graphene(002) [34,35,36] can also be clearly seen on the XRD pattern of the CuAlNi-C alloy and this is a confirmation both for the existence of graphene in the alloy and for the aforementioned remark made upon the little oxygen content (formed by the oxidation of graphene and alloying metal elements) appeared in EDX result.

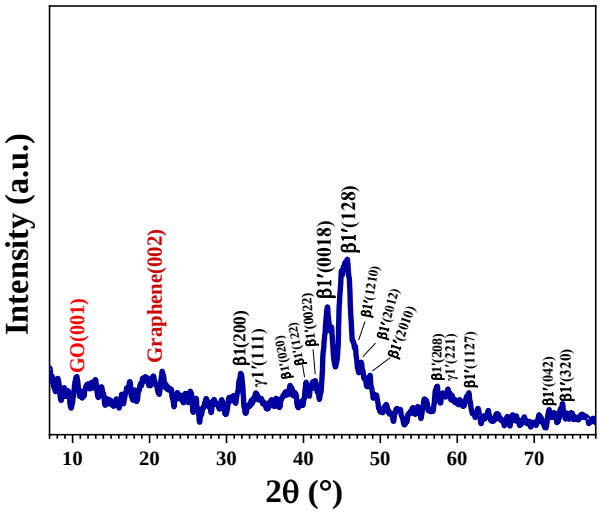

Fig.4. The XRD pattern of CuAlNi-C alloy revealing the diffraction peaks of the different planes of β1'and γ1' martensite phases and graphene and graphene-oxide (GO) forms.

4. Conclusions

In this work the graphene doped CuAlNi-C high temperature shape memory alloy was succesfully produced by arc melting method.

The SEM(+EDX) result showed that the added graphene nanoplatelets were generally distributed homogenously but in localized regions in the alloy, this resulted propably from the usage of inadequate graphene content. A very little oxygen entity was also observed on the EDX result, formed by oxidation of both surfical metal alloying elements and some graphene and this was confirmed by XRD result.

The XRD peaks indicating the existence of the martensite phases as being the base of shape memory effect property of the alloy, and the peaks belonging to the graphene and graphene-oxide (GO) contents were observed on the XRD pattern of the alloy. Besides, the microstructural XRD result revealed that the polycrystalline alloy has both β1'(M18R) type and γ1'(2H) type martensites with various orientations.

The DTA tests showed that the alloy's characteristic martensitic transformation temperatures (found between ~190-379 °C averagely) are far above 100 °C, which classifies the produced alloy as a high temperature shape memory alloy (HTSMA). The multistage phase transitions occurred on each heating fragments of DTA curves as; β1'→β1→B2→precipitations(α+γ2)→eutectoid→B2(ordered) →A2(disordered) showed that the alloy has a high temperature behavior which is common in Cu-based alloys.

The thin graphene nanoplatelets with large (microscale) lateral surface area distributed in the alloy matrix create interfaces between graphene and CuAlNi base alloy matrix, which might have reduced the speed of heat transfer and cause a large hysteresis gap. In conclusion, by doping shape memory alloys with minor amount graphene the characteristic transformation temperatures, shape memory effect, and microstructural properties of shape memory alloys may be sensitively controlled. Moreover, the fabricated graphene doped CuAlNi-C alloy can be useful in HTSMA related applications.

Acknowledgement

This research work financially supported by **FÜBAP, Project No: FF.21.14** is a part of Ph.D. thesis works of Oktay KARADUMAN supervised by Assoc. Prof. Dr. Canan Aksu CANBAY at Firat University, Faculty of Science, Department of Physics. This work is presented in MSNG 2021 International Conference.

References

[1] Otsuka, K., & Wayman, C. M. (Eds.). (1999). *Shape memory materials*. Cambridge university press.

[2] Dasgupta, R. (2014). A look into Cu-based shape memory alloys: Present scenario and future prospects. Journal of Materials Research, **29**(16), 1681-1698. https://doi.org/10.1557/jmr.2014.189

[3] Jani, J. M., Leary, M., Subic, A., & Gibson, M. A. (2014). A review of shape memory alloy research, applications and opportunities. Materials & Design (1980-2015), **56**, 1078-1113. https://doi.org/10.1016/j.matdes.2013.11.084

[4] Al-Humairi, S. N. S. (2020). Cu-based shape memory alloys: modified structures and their related

properties. *Recent Advancements in the Metallurgical Engineering and Electrodeposition*, 25. http://dx.doi.org/10.5772/intechopen.86193

[5] Canbay, C. A., Karaduman, O., & Özkul, İ. (2020). Lagging temperature problem in DTA/DSC measurement on investigation of NiTi SMA. Journal of Materials Science: Materials in Electronics, **31**(16), 13284-13291. https://doi.org/10.1007/s10854-020-03881-y

[6] Frenzel, J. (2020). On the importance of structural and functional fatigue in shape memory technology. Shape Memory and Superelasticity, **6**(2), 213-222. https://doi.org/10.1007/s40830-020-00281-3

[7] Chen, H., Xiao, F., Liang, X., Li, Z., Li, Z., Jin, X., ... & Fukuda, T. (2019). Improvement of the stability of superelasticity and elastocaloric effect of a Ni-rich Ti-Ni alloy by precipitation and grain refinement. Scripta Materialia, **162**, 230-234. https://doi.org/10.1016/j.scriptamat.2018.11.024

[8] Raju, T.N., Sampath, V. (2011). Effect of Ternary Addition of Iron on Shape Memory Characteristics of Cu-Al Alloys. J. of Materi Eng and Perform **20**, 767–770. https://doi.org/10.1007/s11665-011-9916-1

[9] C.A. Canbay, M. Ali Çiçek, Oktay Karaduman, İskender Özkul, Memet Şekerci. (2019). Investigation of Thermoelastical Martensitic Transformations and Structure in New Composition of CuAlMnTi Shape Memory Alloy. JOURNAL OF MATERIALS AND ELECTRONIC DEVICES, **1**(1), 60-64. Retrieved from http://dergi-fytronix.com/index.php/jmed/article/view/45

[10] Karaduman, O., Özkul, I., Altın, S., Altın, E., Bağlayan, Ö., & Canbay, C. A. (2018, November). New Cu-Al based quaternary and quinary high temperature shape memory alloy composition systems. In AIP Conference Proceedings (Vol. **2042**, No. 1, p. 020030). AIP Publishing LLC. https://doi.org/10.1063/1.5078902

[11] Karaduman, O.; Aksu Canbay, C.; Özkul, İ.; Aziz Baiz, S.; Ünlü, N. Production and Characterization of Ternary Heusler Shape Memory Alloy With A New Composition. J. mater. electron. device. 2018, **1**, 16-19. http://dergi-fytronix.com/index.php/jmed/article/download/24/72

[12] Karaduman, O., Ünlü, N., Canbay, C. A., Özkul, İ., & Baiz, S. A. (2018). The Investigation of SME in a Cu-Al-Ni HTSMA. JOURNAL OF MATERIALS AND ELECTRONIC DEVICES, **1**(1), 6-10. http://dergi-fytronix.com/index.php/jmed/article/view/22

[13] Canbay, C. A., Karaduman, O., Ünlü, N., Baiz, S. A., & Özkul, İ. (2019). Heat treatment and quenching media effects on the thermodynamical, thermoelastical and structural characteristics of a new Cu-based quaternary shape memory alloy. Composites Part B: Engineering, **174**, 106940. https://doi.org/10.1016/j.compositesb.2019.106940

[14] Canbay, C. A., Karaduman, O., & Özkul, İ. (2019). Investigation of varied quenching media effects on the thermodynamical and structural features of a thermally aged CuAlFeMn HTSMA. Physica B: Condensed Matter, **557**, 117-125. https://doi.org/10.1016/j.physb.2019.01.011

[15] Karaduman, O., Canbay, C. A., Ünlü, N., & Özkul, İ. (2019, November). Analysis of a newly composed Cu-Al-Mn SMA showing acute SME characteristics. In AIP Conference Proceedings (Vol. **2178**, No. 1, p. 030039). AIP Publishing LLC. https://doi.org/10.1063/1.5135437

[16] López-Ferreño, I., Gómez-Cortés, J. F., Breczewski, T., Ruiz-Larrea, I., Nó, M. L., & San Juan, J. M. (2020). High-temperature shape memory alloys based on the Cu-Al-Ni system: design and thermomechanical characterization. Journal of Materials Research and Technology, **9**(5), 9972-9984. https://doi.org/10.1016/j.jmrt.2020.07.002

[17] Sampath, V. (2005). Studies on the effect of grain refinement and thermal processing on shape memory characteristics of Cu–Al–Ni alloys. Smart materials and structures, **14**(5), S253. https://doi.org/10.1088/0964-1726/14/5/013

[18] Saud, S. N., Hamzah, E., Abubakar, T., & Bakhsheshi-Rad, H. R. (2015). Microstructure and corrosion behaviour of Cu–Al–Ni shape memory alloys with Ag nanoparticles. Materials and Corrosion, **66**(6), 527-534. https://doi.org/10.1002/maco.201407658

[19] Chen, L. Y., Xu, J. Q., Choi, H., Pozuelo, M., Ma, X., Bhowmick, S., ... & Li, X. C. (2015). Processing and properties of magnesium containing a dense uniform dispersion of nanoparticles. Nature, **528**(7583), 539-543. https://doi.org/10.1038/nature16445

[20] Lester, B. T., Baxevanis, T., Chemisky, Y., & Lagoudas, D. C. (2015). Review and perspectives: shape memory alloy composite systems. Acta Mechanica, **226**(12), 3907-3960. https://doi.org/10.1007/s00707-015-1433-0

[21] Razooqi, R. N., Razej, K. H., Abdulhameed, A. T., & Irhayyim, S. S. (2018). The physical and mechanical properties of a shape memory alloy reinforced with carbon nanotubes (CNTs). Tikrit Journal of Pure Science, **23**(9), 80-88. http://tjps.tu.edu.iq/index.php/j/article/view/596

[22] Prendota, W., Goc, K., Miyazawa, S., Takasaki, A., Rybicki, D., & Kapusta, C. (2018). Influence of carbon addition to Fe-Mn-Si type alloy on the structure and shape memory effect. Advances in Materials Science and Engineering, Vol. **2018**, Article ID 6950876, 9 pages. https://doi.org/10.1155/2018/6950876

[23] Saud, S. N., Hamzah, E., Abu Bakar, T. A., & Abdolahi, A. (2014). Influence of addition of carbon nanotubes on structure–properties of Cu–Al–Ni shape memory alloys. Materials Science and Technology, **30**(4), 458-464. https://doi.org/10.1179/1743284713Y.0000000379

[24] Lu, G., Wu, T., Yang, P., Yang, Y., Jin, Z., Chen, W., ... & Jiang, M. (2017). Synthesis of high-quality graphene and hexagonal boron nitride monolayer In-plane heterostructure on Cu–Ni alloy. Advanced Science, **4**(9), 1700076. https://doi.org/10.1002/advs.201700076

[25] Chentouf, S. M., Bouabdallah, M., Gachon, J. C., Patoor, E., & Sari, A. (2009). Microstructural and thermodynamic study of hypoeutectoidal Cu–Al–Ni shape memory alloys. Journal of Alloys and Compounds, **470**(1-2), 507-514. https://doi.org/10.1016/j.jallcom.2008.03.009

[26] Kissinger, H. E. (1957). Reaction kinetics in differential thermal analysis. Analytical chemistry, **29**(11), 1702-1706. https://doi.org/10.1021/ac60131a045

[27] Braga, F. D. O., Matlakhov, A. N., Matlakhova, L. A., Monteiro, S. N., & Araújo, C. J. D. (2017). Martensitic transformation under compression of a plasma processed polycrystalline shape memory CuAlNi alloy. Materials Research, **20**, 1579-1592. https://doi.org/10.1590/1980-5373-MR-2016-0476

[28] Bilican D., Kurdi S., Zhu Y., Solsona P., Pellicer E., Barber ZH., Greer AL., Sort J., Fornell J. (2019). Epitaxial Versus Polycrystalline Shape Memory Cu-Al-Ni Thin Films. Coatings, **9**(5): 308. https://doi.org/10.3390/coatings9050308

[29] Saud, S. N., Hamzah, E., Abubakar, T., Bakhsheshi-Rad, H. R., Zamri, M., & Tanemura, M. (2014). Effects of Mn additions on the structure, mechanical properties, and corrosion behavior of Cu-Al-Ni shape memory alloys. Journal of Materials Engineering and Performance, **23**(10), 3620-3629. https://doi.org/10.1007/s11665-014-1134-1

[30] Canbay, C. A., Karaduman, O., Ibrahim, P. A., & Őzkul, İ. (2021). Thermostructural shape memory effect observations of ductile Cu-Al-Mn smart alloy. Advances in Materials Research, **10**(1), 45. http://dx.doi.org/10.12989/amr.2021.10.1.045

[31] Abdillah Sani M. Najib, Safaa N. Saud, Esah Hamzah (2019). Corrosion Behavior of Cu–Al–Ni–xCo Shape Memory Alloys Coupled with Low-Carbon Steel for Civil Engineering Applications. Journal of Bio- and Tribo-Corrosion, **5**: 47. https://doi.org/10.1007/s40735-019-0242-8

[32] Zhang, X., & Liu, Q. S. (2016). Influence of alloying element addition on Cu–Al–Ni high-temperature shape memory alloy without second phase formation. Acta Metallurgica Sinica (English Letters), **29**(9), 884-888. https://doi.org/10.1007/s40195-016-0467-1

[33] Saud, S. N., Hamzah, E., Abubakar, T., & Bakhsheshi-Rad, H. R. (2015). Thermal aging behavior in Cu–Al–Ni–xCo shape memory alloys. Journal of Thermal Analysis and Calorimetry, **119**(2), 1273-1284. https://doi.org/10.1007/s10973-014-4265-6

[34] Gupta, B., Kumar, N., Panda, K., Kanan, V., Joshi, S., & Visoly-Fisher, I. (2017). Role of oxygen functional groups in reduced graphene oxide for lubrication. Scientific reports, **7**(1), 1-14. https://doi.org/10.1038/srep45030

[35] Tang, X., Jan, S. S., Qian, Y., Xia, H., Ni, J., Savilov, S. V., & Aldoshin, S. M. (2015). Graphene wrapped ordered LiNi 0.5 Mn 1.5 O 4 nanorods as promising cathode material for lithium-ion batteries. Scientific reports, 5(1), 1-10. https://doi.org/10.1038/srep11958

[36] Yasin, G., Arif, M., Shakeel, M., Dun, Y., Zuo, Y., Khan, W. Q., ... & Nadeem, M. (2018). Exploring the nickel–graphene nanocomposite coatings for superior corrosion resistance: manipulating the effect of deposition current density on its morphology, mechanical properties, and erosion-corrosion performance. Advanced Engineering Materials, **20**(7), 1701166. https://doi.org/10.1002/adem.201701166